

SUPPLEMENTARY FIGURES

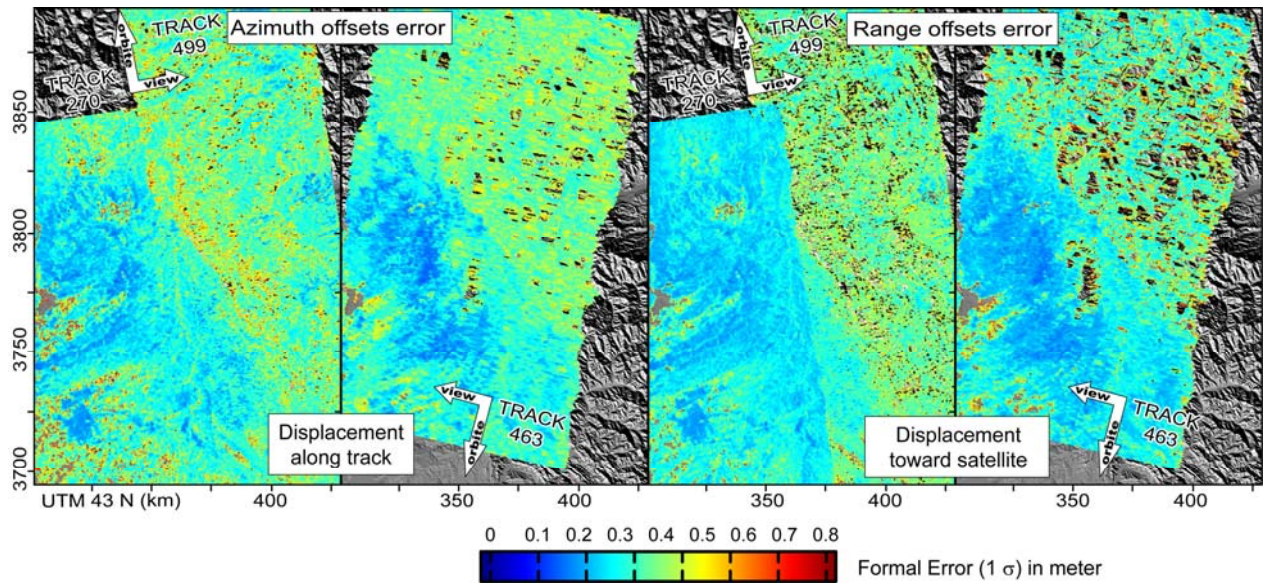


FIGURE S1

Offset errors (one standard deviation) corresponding to data shown in figure 1. Data with errors bigger than one meter have been masked out. These formal errors are based on a measure of the width of the peak in the cross-correlation surface. Errors are usually larger in areas with high relief and steep slopes. Errors also depend of the geometry of acquisition that varies from one track to another. For instance, range offset data for track 270 have lower errors than in the adjacent track 499 due to the smaller baseline of the track 270 (60m vs. 270m). With a baseline about 90 m, but a different Beam Mode (I2, incidence angle at 23° from vertical, instead of I6, at 40° from vertical), the descending track 463 shows similar error to the ascending track 499.

SUPPLEMENTARY FIGURES

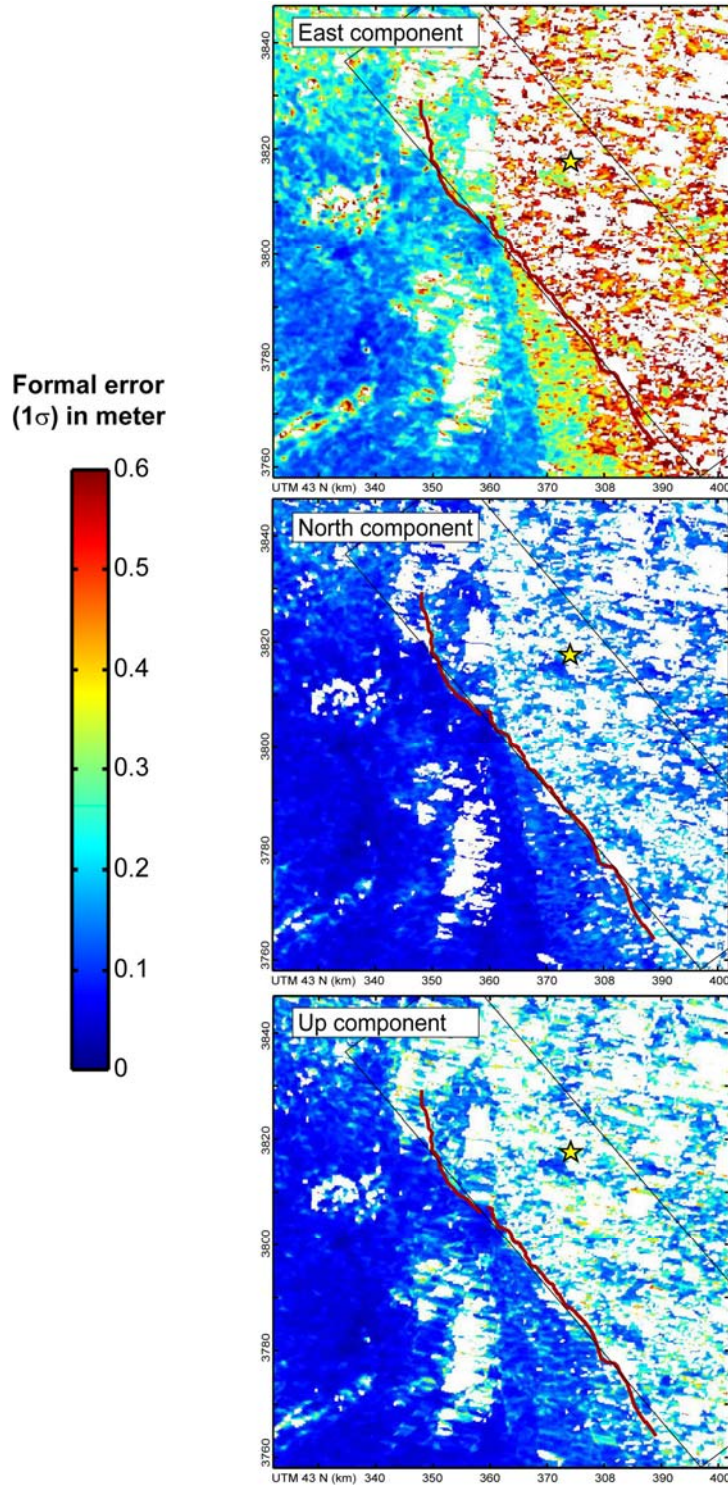


FIGURE S2

3D surface displacement errors propagated from the formal errors of offset data assuming they are independent. The north-south component is the most constrained, whereas the east-west component is less well resolved especially in the eastern part of the studied area, where good quality measurements of the descending track 270 are not available. The red line shows the surface rupture trace, the star is the NEIC epicenter and the thin black lines show the map projection of the plane used to model the fault.

SUPPLEMENTARY FIGURES

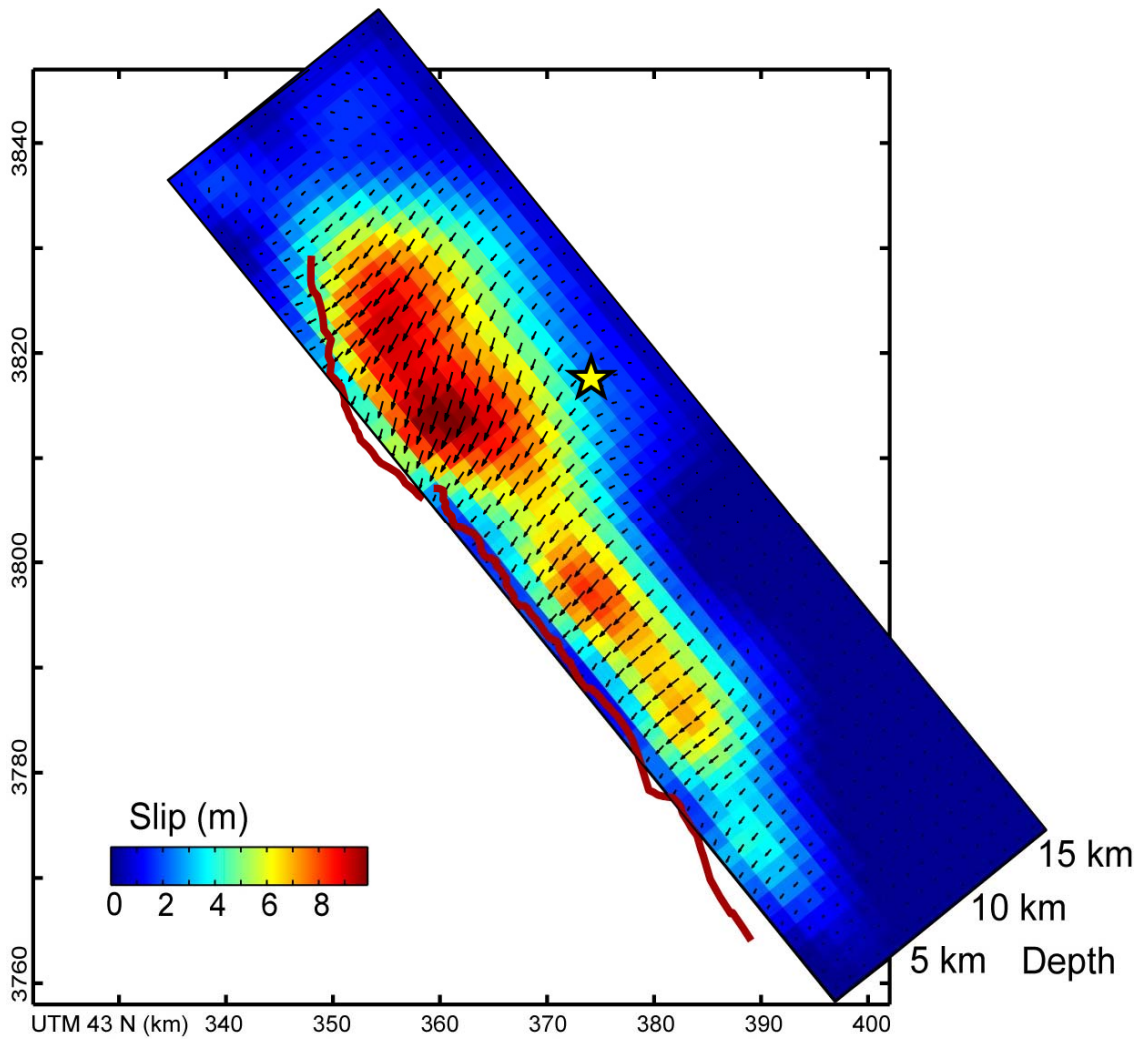


FIGURE S3

Map view of the slip distribution as shown in figure 4. The map frame is the same as in figure 3. Magnitude of displacement is represented by color and slip vectors by the arrows. The red line shows the surface rupture trace. The star is the NEIC epicenter.

SUPPLEMENTARY FIGURES

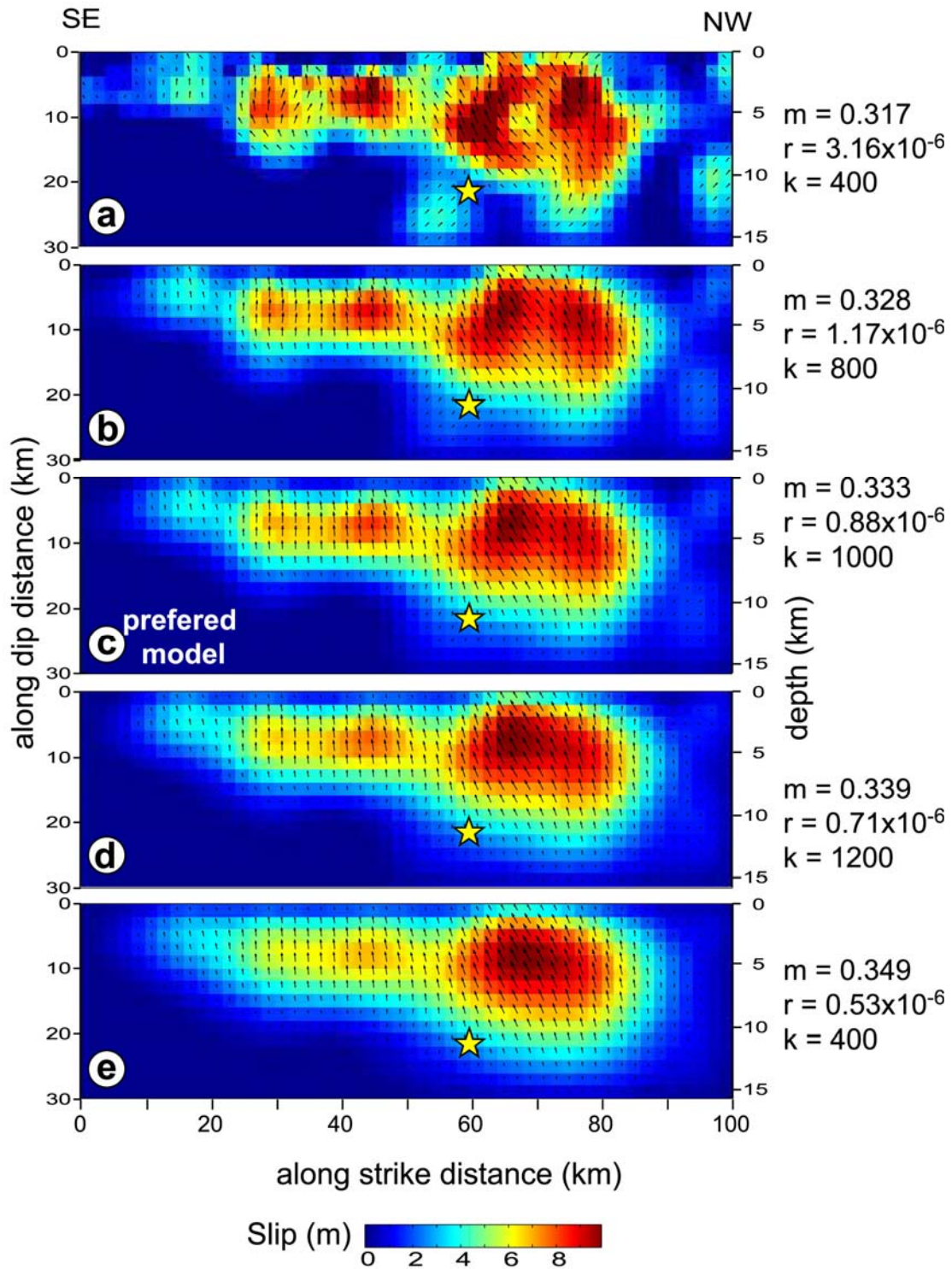


FIGURE S4a

Slip distributions for 5 different smoothness factors (k). In each case, the geometry of the fault plane, the data and the method used for the inversion are the same, but the smoothness factor (a Laplacian smoothing constraint to prevent unrealistic oscillations). From top to bottom increasing smoothness factor is applied. The preferred model (c) corresponds to the one shown in Figure 4. Magnitude of displacement is represented by color and slip vectors by the arrows. The star is the projection on the fault plane of the NEIC epicenter. For each model the misfit to the data (m in meter), the roughness of the model (r) and the smoothness factor applied to the model (k) is given (see Figure S4b for details).

SUPPLEMENTARY FIGURES

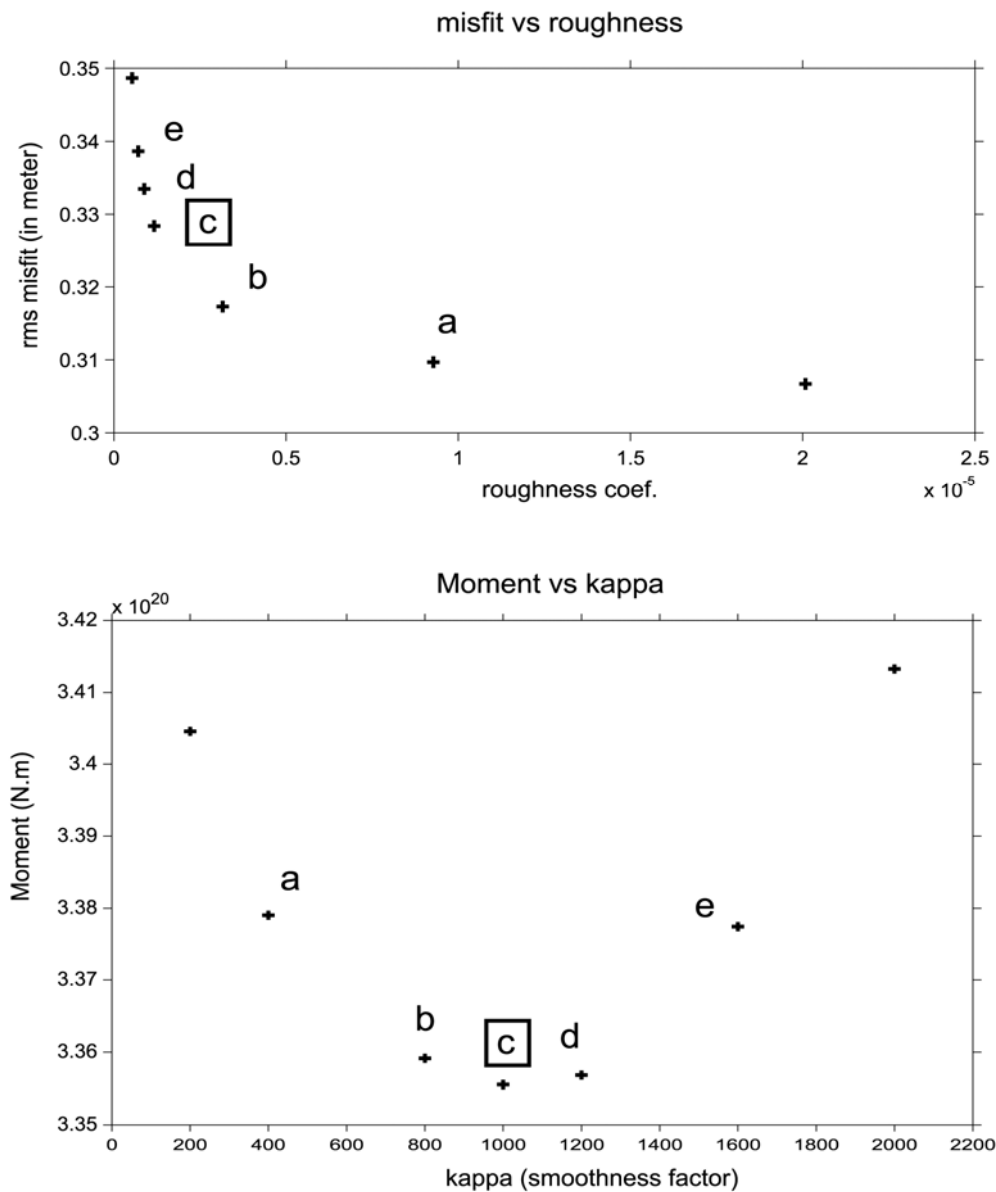


FIGURE S4b

Choice of smoothness factor for slip distribution. In both graphs, the letters correspond to the models shown in figure S4a, and the black square indicates the preferred model.

Top: RMS misfit to the data used in the inversion (data downsampled to about 2000 points for each of the 6 offset datasets using a quad-tree algorithm) versus roughness of the model (defined as the mean absolute Lapacian) for different value of the smoothness factor. Increasing the smoothness factor leads to a decrease in roughness at the cost of increasing misfit. For low smoothness, the fit to the data is better but the solution shows unreasonable slip patterns inherent to the inversion scheme (e.g. *Du et al. 1992* *). The best trade-off is between model b and c. As the choice between the two models is quite subjective, we used another criterion to choose one of the two models, that is the minimization of the seismic moment (see bottom figure).

Bottom: Seismic moment for each model versus the smoothness factor applied to each model. We used the model with the minimum seismic moment to choose between solutions b and c.

* *Du, Y., A. Aydin, and P. Segall (1992). Comparison of various inversion techniques as applied to the determination of a geophysical deformation model for the 1983 Borah Peak earthquake, Bull. Seism. Soc. Am. 82, 1840–1866.*

SUPPLEMENTARY FIGURES

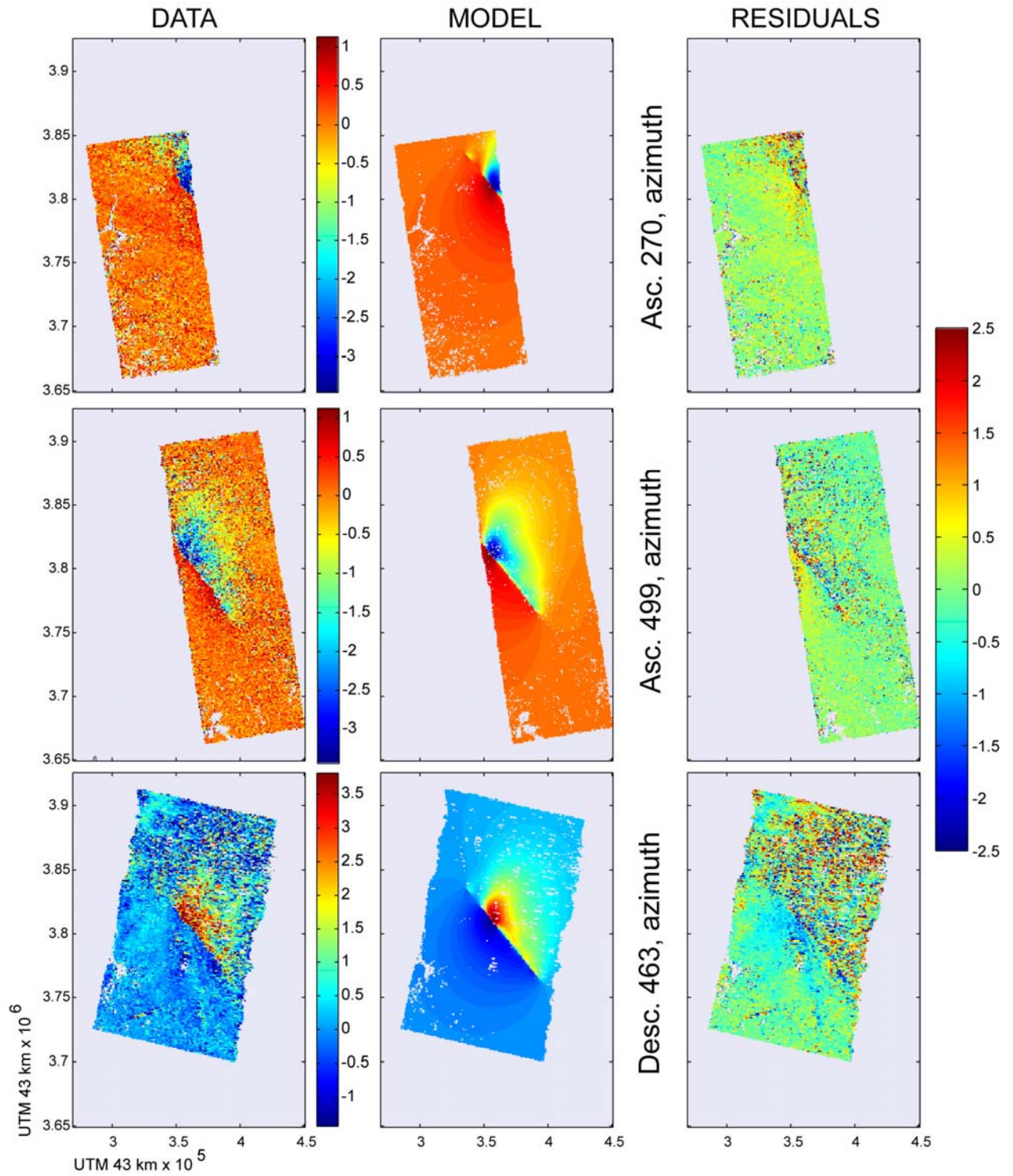


FIGURE S5a

Residuals of the slip distribution model (model minus data). For each dataset (each row), the offset data and offset constructed from the slip distribution model are shown with the same color scale (in meter). The right column shows the corresponding residuals.

SUPPLEMENTARY FIGURES

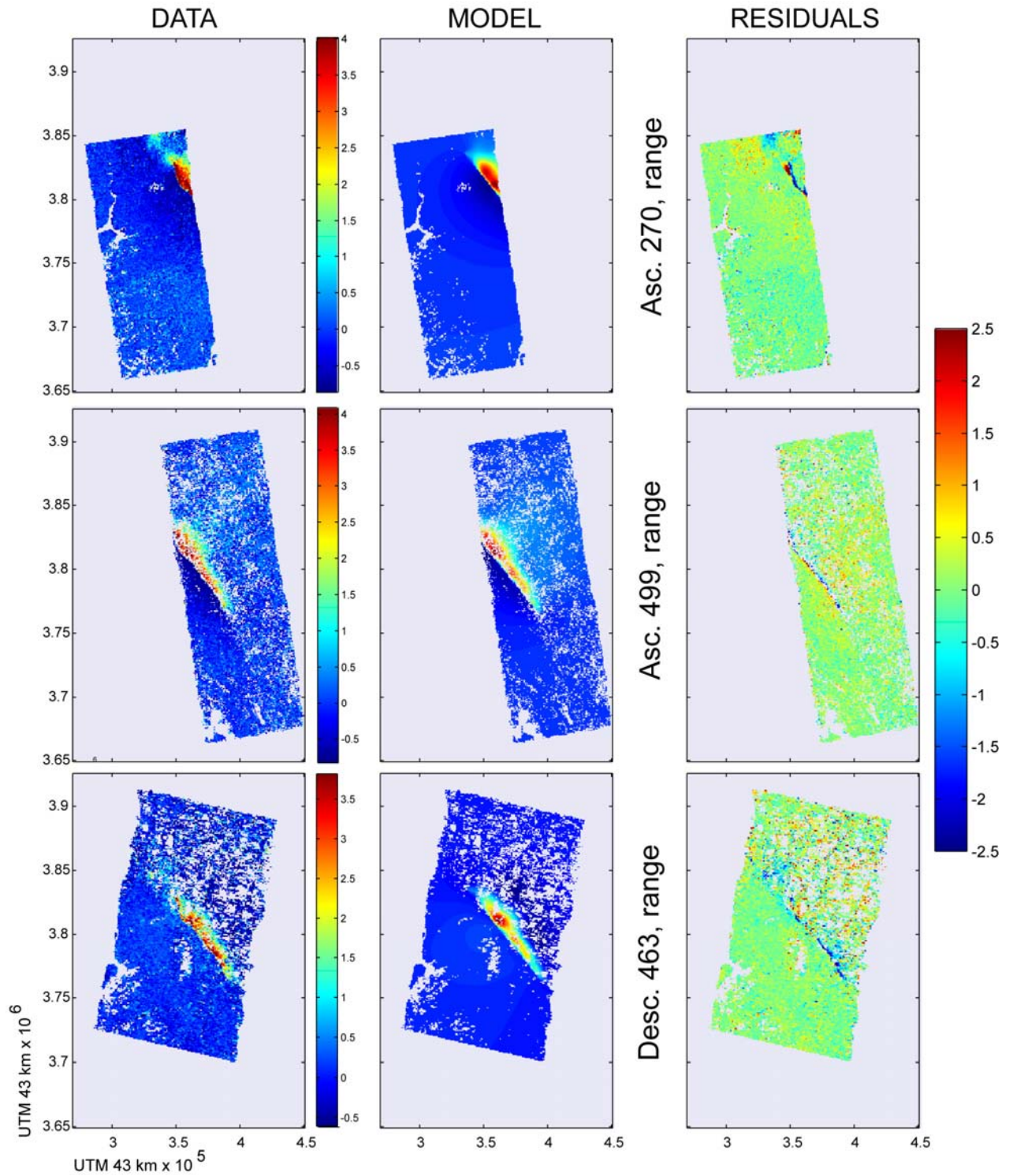


FIGURE S5b

Residuals of the slip distribution model (model minus data). For each dataset (each row), the offset data and offset constructed from the slip distribution model are shown with the same color scale (in meter). The right column shows the corresponding residuals (from -2 to 2 meters).

SUPPLEMENTARY FIGURES

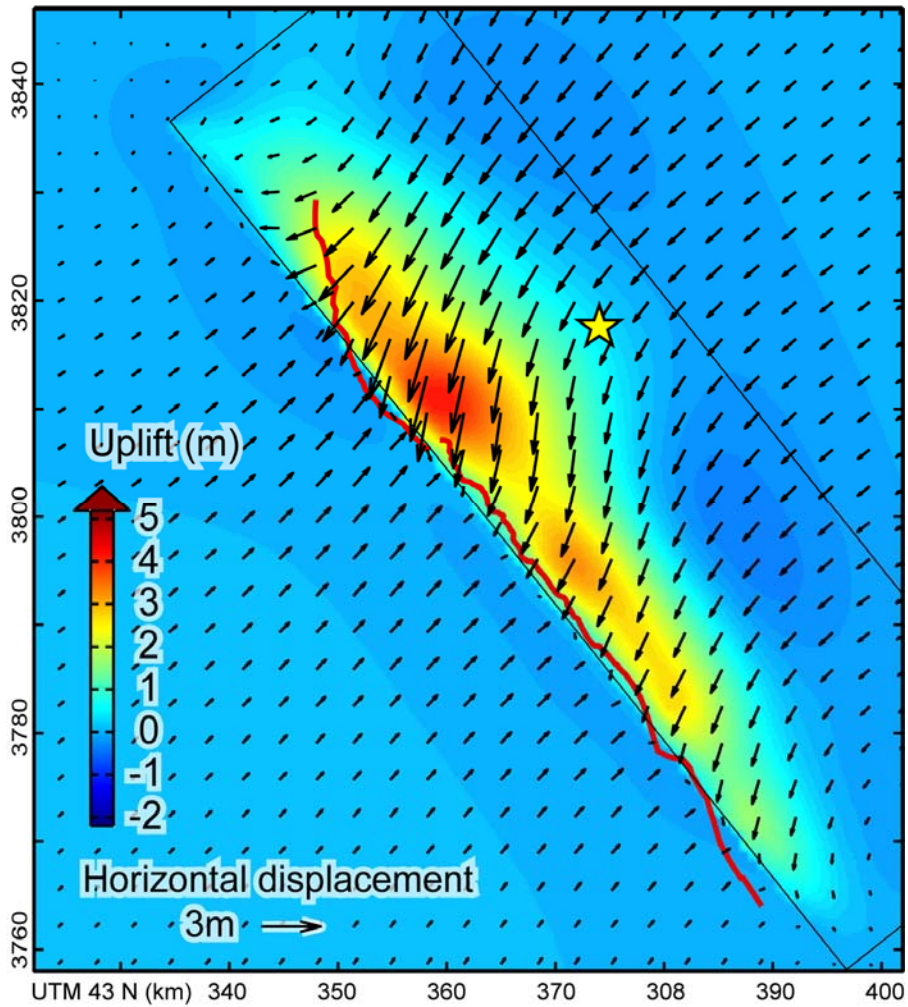


FIGURE S6

3D surface displacement field constructed from the slip distribution model (compare with figure 3). Arrows indicate horizontal displacements, and colors vertical displacements. The red line shows the surface rupture trace, the star is the NEIC epicenter and the thin dark black lines show the map projection of the plane used to model the fault.

SUPPLEMENTARY FIGURES

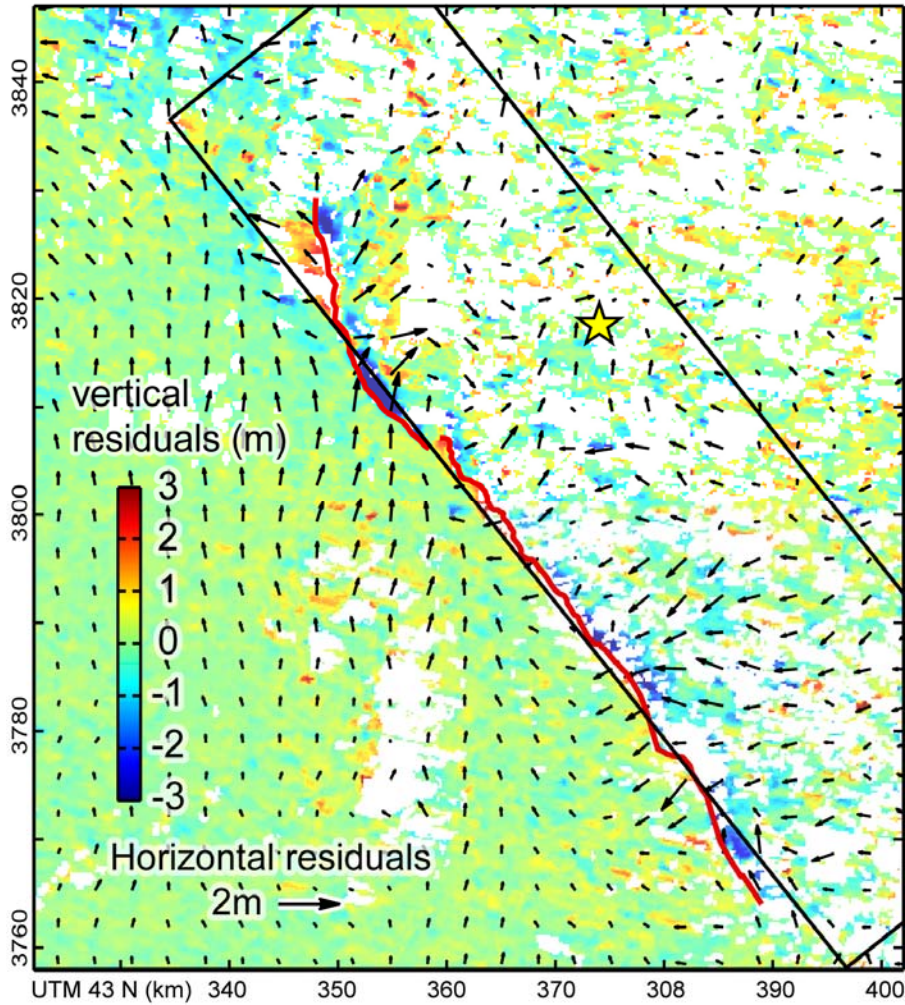


FIGURE S7

Residuals of the 3D surface displacement field constructed from the slip distribution model (figure S6) with respect to the one constructed from the offset data (figure 3). Colors indicate vertical residuals and arrows indicate horizontal residuals. The red line shows the surface rupture trace, the star is the NEIC epicenter and the black lines show the map projection of the plane used to model the fault.

SUPPLEMENTARY FIGURES

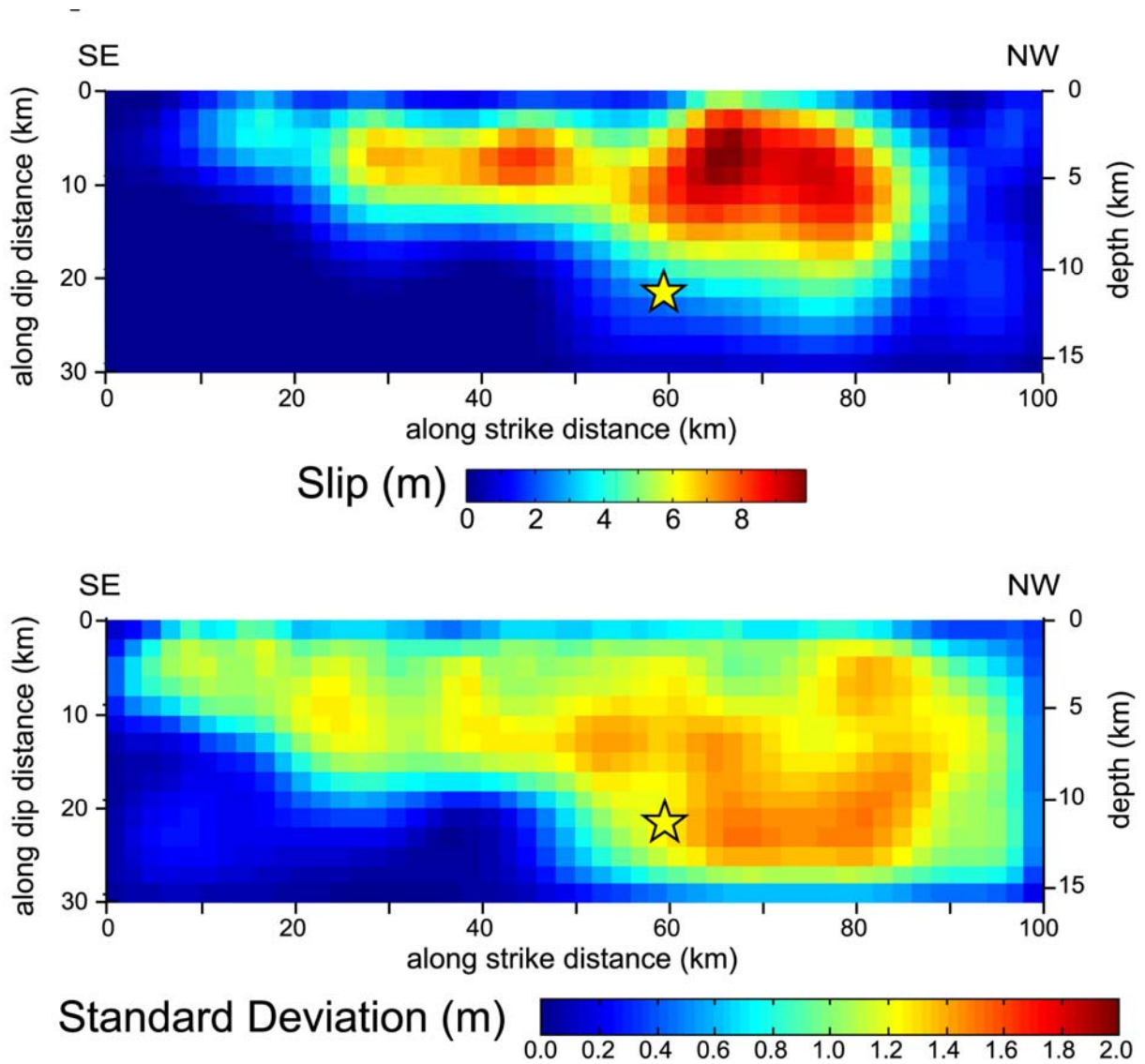


FIGURE S8

Estimation of the model error.

Top: for reference, the slip distribution of the preferred model.

Bottom: Standard deviation of the slip magnitude calculated from 100 solutions using the same inversion procedure and perturbed datasets. The standard deviation of the solutions gives a measure of the error on the amount of slip on each element. The 100 perturbed datasets are created by adding noise (with similar spatial correlation than the noise present in the far field of the original data) to the original dataset (Funning et al. [2005], Appendix B).